

## Deletion of a single mevalonate kinase (*Mvk*) allele yields a murine model of hyper-IgD syndrome

E. J. Hager · H. M. Tse · J. D. Piganelli · M. Gupta ·  
M. Baetscher · T. E. Tse · A. S. Pappu · R. D. Steiner ·  
G. F. Hoffmann · K. M. Gibson

Received: 19 September 2007 / Submitted in revised form: 9 October 2007 / Accepted: 10 October 2007 /  
Published online: 19 November 2007  
© SSIEM and Springer 2007

**Summary** In the current study our objective was to develop a murine model of human hyper-IgD syndrome (HIDS) and severe mevalonic aciduria (MA), auto-inflammatory disorders associated with mevalonate kinase deficiency (MKD). Deletion of one *Mvk* allele (*Mvk*<sup>+/-</sup>) yielded viable mice with significantly reduced liver *Mvk* enzyme activity; multiple matings failed to produce *Mvk*<sup>-/-</sup> mice. Cholesterol levels in

tissues and blood, and isoprene end-products (ubiquinone, dolichol) in tissues were normal in *Mvk*<sup>+/-</sup> mice; conversely, mevalonate concentrations were increased in spleen, heart, and kidney yet normal in brain and liver. While the trend was for higher IgA levels in *Mvk*<sup>+/-</sup> sera, IgD levels were significantly increased (9–12-fold) in comparison to *Mvk*<sup>+/+</sup> littermates, in both young (<15 weeks) and older (>15 weeks) mice. *Mvk*<sup>+/-</sup> animals manifested increased serum TNF- $\alpha$  as compared to wild-type littermates, but due to wide variation in levels between individual *Mvk*<sup>+/-</sup> mice the difference in means was not statistically significant. *Mvk*<sup>+/-</sup> mice represent the first animal model of HIDS, and should prove useful for examining pathophysiology associated with this disorder.

---

Communicating editor: Johannes Zschocke

---

Competing interests: None declared

---

References to electronic databases: Mevalonate kinase: EC 2.7.1.36; OMIM 610377;251170;260920.

---

This paper has been presented in abstract form (Gibson et al 2006, 2007).

---

E. J. Hager · T. E. Tse · K. M. Gibson (✉)  
Division of Medical Genetics, Children's Hospital  
of Pittsburgh, University of Pittsburgh School of Medicine,  
Rangos Research Building, Room 2113, 3460 Fifth Ave.,  
Pittsburgh, PA 15213, USA  
e-mail: michael.gibson@chp.edu

H. M. Tse · J. D. Piganelli  
Division of Immunogenetics, Department of Pediatrics,  
Children's Hospital of Pittsburgh, University of Pittsburgh  
School of Medicine, Pittsburgh, PA, USA

M. Gupta · M. Baetscher · R. D. Steiner  
Department of Molecular and Medical Genetics,  
Oregon Health & Science University, Portland, OR, USA

M. Baetscher  
Department of Comparative Medicine,  
Oregon Health & Science University, Portland, OR, USA

A. S. Pappu  
Department of Medicine,  
Oregon Health & Science University, Portland, OR, USA

R. D. Steiner  
Department of Pediatrics,  
Oregon Health & Science University, Portland, OR, USA

R. D. Steiner  
Oregon Clinical and Translational Research Institute,  
Oregon Health & Science University, Portland, OR, USA

G. F. Hoffmann  
Department of Pediatrics, University of Heidelberg,  
Heidelberg, Germany

K. M. Gibson  
Department of Pathology, Biochemical Genetics/  
Nutrition Laboratory, University of Pittsburgh  
School of Medicine, Pittsburgh, PA, USA

*Present Address:*

M. Baetscher  
Genome Manipulation Facility,  
Harvard Stem Cell Institute and Department  
of Molecular and Cellular Biology,  
Harvard University, Cambridge, MA, USA

**Abbreviations**

- FDP farnesyl diphosphate
- GGDP geranylgeranyl diphosphate
- HIDS human hyper-IgD syndrome
- MA mevalonic aciduria
- MKD mevalonate kinase deficiency
- PBMC peripheral blood mononuclear cell
- PCC propionyl-CoA carboxylase

**Introduction**

Mevalonate kinase (MVK; EC 2.7.1.36; OMIM 610377;251170;260920), a cytosolic enzyme involved in early cholesterol and nonsterol isoprene formation (Fig. 1), is also the locus for human defects with diverse phenotypes, including severe mevalonic aciduria (MA) (Hoffmann et al 1986) and hyperimmunoglobulinaemia D (hyper-IgD syndrome; HIDS) (Drenth et al 1994, 1999). Clinically, MA and HIDS are distinguishable based upon the extent of neurological involvement, including cerebellar atrophy, psychomotor retardation, ataxia and dysmorphic features in MA patients, while most HIDS patients do not manifest neurological disease (Prietsch et al 2003). Both disorders may present with hepatosplenomegaly, lymphadenopathy, anaemia, increased erythrocyte sedimentation rates and levels of C-reactive protein, leukocytosis, and increased urinary leukotriene excretion. HIDS patients suffer recurrent febrile episodes throughout their life-

time characterized by elevated serum IgD and IgA1 levels, skin rash, arthritis, arthralgia and myalgia.

It has been hypothesized that the more severe MA clinical presentation correlates with lower residual MVK activity and more severe pathogenic gene mutations (Mandey et al 2006a). Experimental data are in concordance with this hypothesis. HIDS patients manifest higher residual MVK enzyme activity (1–8% of control) than MA patients (~0.1% of control). Genotype analysis suggests further divergence between the disorders. Human MVK is located on chromosome 12q24, and ~63 pathological sequence variations have been reported throughout its 10 coding exons (Mandey et al 2006a). Of these mutations, two alleles appear more prevalent, c.803T>C (p.I268T) and c.1129G>A (p.V377I), the latter almost exclusively associated with HIDS patients. The V377I mutation has been observed with high frequency in the Dutch population, and is a variation that confers temperature sensitivity to the MVK protein. MVK activity in cultured fibroblasts derived from HIDS patients harbouring the V377I allele displayed substantially higher MVK activities at 30°C vs 37°C, while MVK activity in peripheral blood mononuclear cells decreased 2- to 8-fold when HIDS patients experienced febrile attacks. Accordingly, Houten and co-workers have suggested that minor temperature elevations in HIDS patients result in MVK activity that is rate-limiting in pathway function, associated with temporary deficiency of isoprene end-products and a concomitant induction of inflammation and fever

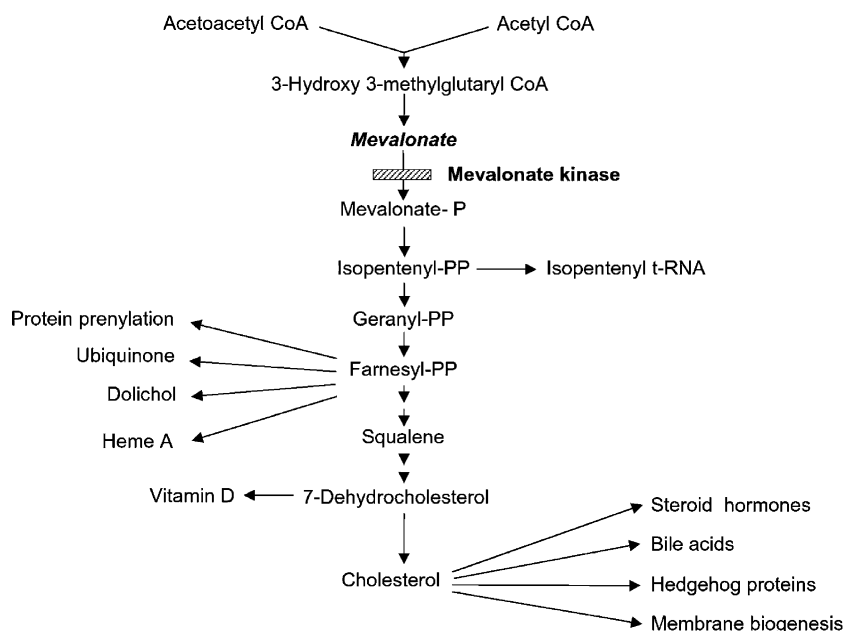


**Fig. 1** Mevalonate pathway in mammalian cells (not all steps are shown). The site of the defect in patients with MA and HIDS is mevalonate kinase, which follows the highly-regulated step of

HMG-CoA reductase activity. Mevalonate-P, mevalonate-5-phosphate; PP, diphosphate; t-RNA, transfer RNA

(Houten et al 2002). The findings of Rios and co-workers, however, are discordant with the purported role of the V377I allele (Rios et al 2001). These investigators reported that valine-377 is not invariant in several eukaryotic MVK amino acid sequences, is greater than 18 Å in distance from the active site, and does not produce a recombinant protein with substantially reduced MVK activity or temperature sensitivity.

Human MKD has been categorized as an auto-inflammatory disease characterized by systemic inflammation without an apparent infectious aetiology (Mandey et al 2006a). MVK-deficient patients exhibit dysregulation of IL-1 $\beta$ , a major inflammatory cytokine. Stimulated peripheral blood mononuclear cells (PBMCs) cultured from MVK-deficient patients hypersecrete IL-1 $\beta$ , a process that is exacerbated by addition of lovastatin and potentially linked to a shortage of geranylgeranylated proteins (Mandey et al 2006b). To begin examining the pathophysiology associated with MA and HIDS, we have partially ablated *Mvk* in the mouse and pursued preliminary immunological and biochemical characterization. The current report summarizes our findings.

## Materials and methods

### Gene targeting and animal husbandry

The murine *Mvk* gene was ablated employing a gene trap-disrupted mouse embryonic stem (ES) cell line (OST 201716, Lexicon Pharmaceuticals, The Woodlands, TX, USA) as described elsewhere (Hogema et al 2001). Chimeric mice were obtained by ES cell injection into blastocysts from strain C57BL/6, followed by implantation of injected embryos into pseudopregnant females for development to term. Male chimeras showing extensive ES cell-derived agouti coat color were bred with C57BL/6

females for germline transmission. Mouse protocols were approved by the Animal Research & Care Committee, Children's Hospital of Pittsburgh, and mice were housed in a specific pathogen-free (spf) facility.

The Omnibank gene trap vector (Lexicon Pharmaceuticals) was located within intron 1 of the *Mvk* coding region on mouse chromosome 5 (BC005606; *Mus musculus Mvk*; <http://genome.ucsc.edu>) between nucleotides 111857411 and 111857412. Genotyping was performed using a three-primer PCR reaction (forward 5'-wild-type, 5'-GCT CTG GAT GGT AGT TCT GGA-3' corresponding to chr. 5 nucleotides 111857415–435; forward 5'-mutant, 5'-AAA TGG CGT TAC TTA AGC TAG-3', corresponding to 21 nucleotides of the Omnibank vector sequence; and reverse 3'-wild-type, 5'-CTT GCC ATG GAC CAC AGC GT-3', corresponding to chr. 5 nucleotides 111857738–757). PCR reactions were carried out in 0.05 ml final volume supplemented with 0.3  $\mu$ mol/L of each primer, 5  $\mu$ l 10 $\times$  PCR buffer, 300  $\mu$ mol/L dNTPs, 2.5 U Taq, and 2  $\mu$ l DNA solution from tail clips. Tail clips were obtained at weaning, and nucleic acid was obtained by salt extraction. PCR cycling conditions were: 95°C, 5 min; 33 cycles of 94°C, 1 min; 52°C, 2 min; 72°C, 3 min; followed by 72°C, 7 min and finally 4°C until analysis. Samples were electrophoresed on a 1.2% agarose gel for 45 min at 110 V. Bands were visualized by ethidium bromide staining (wild-type, 342 bp; mutant, 222 bp). For a schematic diagram of primer locations and gene trap insertion site, see Fig. 2. Since multiple heterozygous matings (*Mvk*<sup>+/-</sup>  $\times$  *Mvk*<sup>+/-</sup>) failed to produce a complete knockout (*Mvk*<sup>-/-</sup>; >100 matings) we assumed embryonic lethality and instituted a breeding scheme to maximize production of *Mvk*<sup>+/-</sup> mice for characterization. To date, we have not characterized the time-point of embryonic lethality, nor analysed the embryos themselves, choosing to focus our primary attention on immunological features of the *Mvk*<sup>+/-</sup> mice.

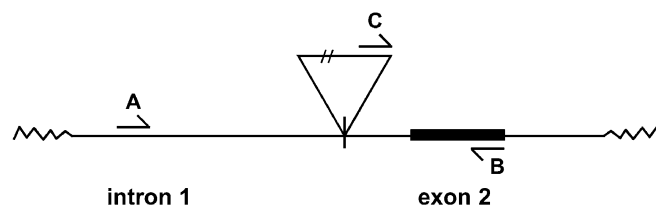


**Fig. 2** Schematic diagram of the genomic *Mvk* structure in the mouse, location of the gene trap employed to disrupt *Mvk* activity, and location/orientation of primers for PCR analysis and genotyping. The 5' forward primer (A) annealing site is between bases 851 and 871 in intron 1 of the *Mvk* locus and is positioned 170 bp upstream of the gene trap cassette insertion site (triangle). The 3' reverse primer (B) anneals between bases

1174 and 1193 in exon 2, which is 172 bp downstream of the insertion site. The PCR product amplified from the wild-type allele is 342 nucleotides (nt) in length. The gene trap cassette inserts 5176 bp at position 1021 in intron 1 of the *Mvk* locus. The 5' forward primer (C) annealing site is 50 bases from the 3' end of the 3' LTR region of the insertion cassette. Primers B and C amplify a 222 nt product from the mutant allele

## Enzymology and metabolite quantitation

*Mvk* and the control enzyme, propionyl-CoA carboxylase (PCC), activities were quantified in liver homogenates as described (Gibson et al 1988). For mevalonate quantification, tissues were weighed and sonicated in 1 ml of 20 mmol/L potassium phosphate buffer pH 7.4 with 1 mmol/L DTT to obtain a uniform suspension. The tissue suspension was centrifuged at 105,000 *g* for 1 h. Ultrafiltrates were prepared from the resulting supernatant using Amicon Ultra-free-CL filters (Pappu et al 1989, 2006). The concentration of mevalonate in ultrafiltrates was determined by mevalonate phosphorylation using purified recombinant mevalonate kinase. Tissue ubiquinone was extracted by a modified method of Okamoto et al (1988) with HPLC employing a reversed-phase Phenomenex 3  $\mu$ m (C18) column and methanol–hexane (90:10 v/v) as the mobile phase (Pappu et al 2006). Dolichol was extracted from tissues and separated from other lipids using C18 Seppak cartridges (Waters). The isolated dolichol was measured by HPLC employing a Phenomenex 3  $\mu$ m (C18) column and 2-propanol–methanol (72:28 v/v) as the mobile phase (Pappu et al 2006; Turpeinen 1986). Cholesterol was extracted from tissues using chloroform–methanol (2:1 v/v) and quantified enzymatically (Roche Diagnostics).

## Immunological determinations

Serum IgA levels were quantitated according to the manufacturer's instructions using the Beadlyte Mouse Immunoglobulin Isotyping Kit/Luminex Technology (Upstate, Charlottesville, VA, USA). Serum IgD was assayed by standard sandwich ELISA technique. Briefly, 96-well plates (Nunc Maxisorp; Nalge Nunc, Rochester, NY, USA) coated with 100  $\mu$ l/well of 2  $\mu$ g/ml anti-IgD antibody (eBioscience, clone 11–26; San Diego, CA, USA) diluted in 10 mmol/L PBS were incubated overnight at 4°C. The plates were washed three times/5 min each in PBS-Tween 20 (0.02%) (PBST), blocked in 1% BSA for 1 h at room temperature, and washed as above. Serum dilutions in 0.7% BSA were plated in 100  $\mu$ l/well volumes at 1:10 and 1:50, followed by two-fold serial dilutions thereafter, incubated overnight at 4°C, and washed as described. One-hundred  $\mu$ l/well horseradish peroxidase (HRP)-labelled anti-IgD antibody (American Research Products, clone MD-6; Belmont, MA, USA) was added to wells diluted 1:1000 in 0.7% BSA and incubated at room temperature for 2 h. Plates were washed extensively prior to the addition of 100  $\mu$ l/well ABTS peroxidase substrate (KPL, Gaithersburg, MD, USA). Following 45 min of

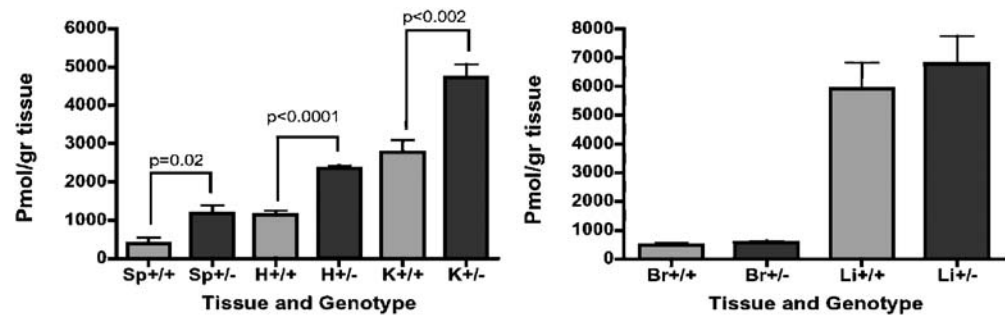
colour development, absorbance was measured at 405 nm. Positive serum titres of IgD were determined to be those above background reagent controls and levels of pooled normal mouse serum (Abcam, Cambridge, MA, USA) titrated likewise that essentially had no detectable reactivity in our ELISA. TNF- $\alpha$  was assayed by ELISA essentially as described above. Antibody pairs (clone TN3-19/anti-TNF- $\alpha$ -biotin, rat polyclonal) were purchased (eBioscience) and used at concentrations according to the manufacturer's recommendations. Streptavidin conjugated to HRP (BD Biosciences; San Jose, CA, USA), a second-step reagent for detection of biotinylated antibodies, was used at a 1:1000 dilution. Positive titres were those considered to be above background reagent controls and titrated pooled normal mouse serum.

## Results

### Enzyme and metabolite results

To verify knockdown, the activities of *Mvk* and the control enzyme PCC were quantified in liver extracts derived from 8 week-old-mice. The ratios of *Mvk*/PCC were: *Mvk*<sup>+/+</sup> (*n*=4), 5.04 $\pm$ 0.83 (*n*=4; SEM); *Mvk*<sup>+/-</sup> (*n*=6), 2.68 $\pm$ 0.72 (*p* < 0.05, one-tailed *t*-test). To determine the effect of gene ablation on mevalonate levels in tissues, mevalonate was quantified in the tissue extract/filtrates employing a radiometric HPLC assay. Using 6 week-old littermates, heart, brain, kidney, spleen and liver were harvested from eight wild-type and six *Mvk* gene-ablated mice. Mevalonate levels in extracts of spleen, heart and kidney were significantly increased in *Mvk*<sup>+/-</sup> animals as compared with *Mvk*<sup>+/+</sup> littermates (Fig. 3), but not significantly altered in liver and brain. Patients with MA have only marginally decreased (or normal) cholesterol levels in serum, while some patients have manifested a decreased level of isoprenes such as ubiquinone (Hubner et al 1993). Accordingly, we examined the effect of *Mvk* ablation on the tissue levels of pathway end-products, namely cholesterol, dolichol and ubiquinone. In these studies, heart, kidney, liver and spleen were examined. In all instances, there was no difference in the levels of end-products between genotypes, indicating that partial ablation of *Mvk* was not in itself sufficient to disrupt *de novo* cholesterol formation or isoprene end-product production. Moreover, blood cholesterol levels were not different between *Mvk*<sup>+/-</sup> and *Mvk*<sup>+/+</sup> animals (data not shown), supporting studies in tissues.

**Fig. 3** Tissue mevalonate concentrations in age-matched (6 week-old) *Mvk*<sup>+/+</sup> and *Mvk*<sup>+/-</sup> animals. H, heart; K, kidney; B, brain; S, spleen; Li, liver. Statistical significance was evaluated using a one-tailed Student's *t* test for unpaired groups



### Immunological findings

For immunological characterization, animals were grouped as <15 weeks of age and >15 weeks of age, the approximate median age for all animals examined, in order to facilitate age-related comparisons. Although IgA levels increased in older animals, there was no significant difference with respect to genotype (Fig. 4). Conversely, IgD titre was significantly elevated in *Mvk*<sup>+/-</sup> animals in comparison to age-matched *Mvk*<sup>+/+</sup> littermates, in both age categories and even within *Mvk*<sup>+/-</sup> as they aged (Fig. 4). TNF- $\alpha$  levels were modestly elevated in *Mvk*<sup>+/-</sup> mice compared with wild-type animals that were <15 weeks of age; this increase was considerably higher for *Mvk*<sup>+/-</sup> mice >15 weeks of age as compared with age-matched wild-type animals (Table 1) but failed to reach statistical significance because of considerable variations in TNF- $\alpha$  levels between individual *Mvk*<sup>+/-</sup> mice.

### Phenotypic characteristics of *Mvk*<sup>+/-</sup> mice

From birth throughout at least 48 weeks, these mice are docile and nonaggressive. Their outward appear-

ance suggests that premature aging is occurring. By 12 weeks of age, their coats are ruffled and dull and their movements are slowed. They are often clearly not 'feeling well' although some individuals do rebound between observations. Upon sacrifice of animals between 20 and 40 weeks of age, about 25% have hepatomegaly with some livers almost doubled in size compared with those of *Mvk*<sup>+/+</sup> littermates. Almost a third of the mice have splenomegaly with spleen sizes ranging 3–4 times larger than those of wild-type. Interestingly, about 20% of these mice have at least one sizeable intestinal polyp in the large bowel, white in colour, and measuring roughly 3–4 cm in length and 1–1.5 cm in width. The inguinal lymph nodes were not observed to be enlarged. The femurs were brittle and marrow was hypocellular with an erythroid dominance and dysplastic megakaryocytes. The peripheral blood smears revealed severe neutropenia with white blood cell differential averages of 74% atypical lymphocytes and 26% monocytes. There was overt basophilic stippling of the red blood cells consistent with the bone marrow observations, suggesting that an anaemic process was occurring. In many aspects, these gross phenotypic observations mirror those observed in human MVK patients.

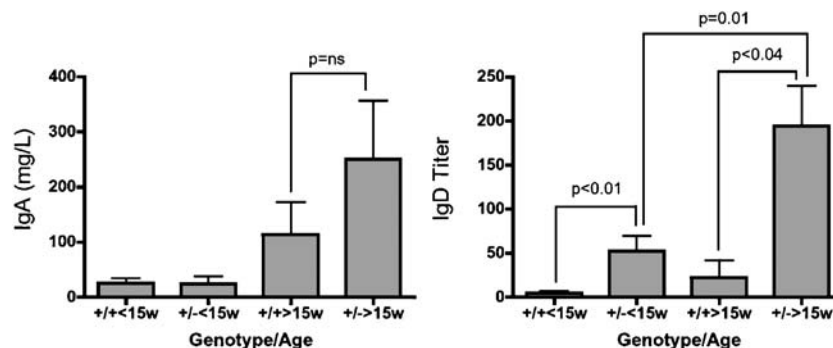


**Fig. 4** Serum IgD titres and IgA concentrations in *Mvk*<sup>+/+</sup> and *Mvk*<sup>+/-</sup> mice (mean $\pm$ SEM). Mean ages: +/+<15 weeks, 8.3 $\pm$ 1.5 (*n*=13); +/+>15 weeks, 25 $\pm$ 5.8 (*n*=16); +/-<15 weeks, 7.5 $\pm$ 1.0 (*n*=11); and +/->15 weeks, 29 $\pm$ 6.9 (*n*=40 mice). There was no

significant difference ( $p>0.05$ ) between mean ages for the subgroups of animals by genotype. Data for all immunoglobulin levels were analysed by one-tailed Student's *t* test analysis

**Table 1** Serum TNF- $\alpha$  cytokines in *Mvk*<sup>+/-</sup> mice as a function of age

| Age       | Genotype                  | TNF- $\alpha$ (pg/ml) <sup>a</sup> | % Positive (no. of animals) <sup>b</sup> |
|-----------|---------------------------|------------------------------------|--|
| <15 weeks | <i>Mvk</i> <sup>+/+</sup> | 96±28                              | 34% (29)                                 |
|           | <i>Mvk</i> <sup>+/-</sup> | 130±55                             | 28% (25)                                 |
| >15 weeks | <i>Mvk</i> <sup>+/+</sup> | 87±60                              | 22% (9)                                  |
|           | <i>Mvk</i> <sup>+/-</sup> | 220±106                            | 35% (17)                                 |

<sup>a</sup> Values are mean±standard error of the mean.

<sup>b</sup> Percent positive refers to the number of animals demonstrating a measurable titre for TNF- $\alpha$  (e.g. 10/29 animals or 34% (*Mvk*<sup>+/+</sup>, <15 weeks of age).

We have conducted limited studies of body temperature in 12 week-old female mice ( $n=2$ , *Mvk*<sup>+/-</sup>;  $n=2$ , *Mvk*<sup>+/+</sup>). Our findings suggest that *Mvk*<sup>+/-</sup> mice have homeostatic thermoregulatory differences from wild-type littermate controls. Mice were implanted with mini-mitters that measured core body temperature over a 48-h span at 10-min intervals at 70°F (21°C) ambient temperature with alternating 12 h cycles of light and dark. Animals were fed *ad libitum*. Body temperatures of both wild-type and *Mvk*<sup>+/-</sup> mice fluctuated rhythmically about a mean temperature, 35.1°C and 36.0°C, respectively, with *Mvk*<sup>+/-</sup> approximately one degree higher. In wild-type mice, the oscillations ranged between 34 and 36°C having a maximal 2 degrees amplitude, while the *Mvk*<sup>+/-</sup> mice ranged between 34 and 38°C having a maximal 4 degrees amplitude. The temperature rhythmicity pattern of wild-type mice showed a rapid fluctuation frequency having an average period length of oscillation of 0.5 min while the *Mvk*<sup>+/-</sup> mice temperature patterns had an average periodicity of 0.9 min, thus a slower fluctuation frequency almost twice as long as that of wild-type. Taken together, these very interesting preliminary findings suggest that loss of a single *Mvk* allele in these mice results in changes in thermoregulation. Further studies are in progress.

## Discussion

Loss of a single *Mvk* allele in the mouse is associated with significant accumulation of tissue mevalonate, notably in spleen, kidney and heart (Fig. 3). However, mevalonate was not elevated in liver and brain, perhaps a reflection of the higher buffering capacity of the latter two organs in mammals (Ness and Chambers 2000). Conversely, the decrease of *Mvk* activity in liver did not appear sufficient to negatively impact end-product formation (cholesterol, dolichol and ubiquinone), which shows parallels with metabolic features of patients with

HIDS and MA. These patients, despite a >90% reduction of MVK activity, have only moderately decreased (or low normal) serum cholesterol levels (Prietsch et al 2003), which may also reflect the effect of exogenous cholesterol uptake via the LDL receptor.

On the other hand, characterization of isoprene end-products (e.g. ubiquinone) in body fluids derived from MA patients has revealed decreased levels (Hubner et al 1993; Prietsch et al 2003). At least in peripheral tissues (blood, fibroblasts), HIDS patients manifest 1–8% residual MVK enzyme activity, while the same residual activity in MA patients is less than 1% (Prietsch et al 2003). Although the percentages are different, a parallel appears to exist in the mouse, in which 50% residual *Mvk* activity results in a HIDS phenocopy (without obvious features of neurological dysfunction), whereas complete loss of gene function appears to be lethal. Previous reports on deletion of specific genes in cholesterol synthesis in the mouse have revealed a high degree of embryonic lethality. Ablation of HMG-CoA reductase (*Hmgcr*<sup>-/-</sup>) and squalene synthase (*SS*<sup>-/-</sup>) genes in mice results in embryonic lethality at E8.5–10.5 (Ohashi et al 2003; Tozawa et al 1999). Embryonic lethality in *Mvk*<sup>-/-</sup> animals, in association with complete abrogation of gene function, is consistent with the above models, and further suggests that alterations of either pre- or post-squalene cholesterol biosynthesis in the mouse are equally deleterious.

Our immunological data on mice with partial ablation of *Mvk* suggests that we have developed an animal model of HIDS which manifests elevations of serum IgD, IgA and TNF- $\alpha$  consistent with those observed in HIDS patients (Klasen et al 2001). The mechanism of autoinflammation in MKD patients and that induced in *Mvk*-ablated mice remains to be defined, but may reside within cell signalling processes and/or lipid raft formation. For example, Ras, Rho and Rab GTPases are isoprenylated proteins actively involved in intracellular signalling pathways whose

activities are dependent upon cell membrane localization. Membrane anchoring is achieved by covalent binding of either farnesyl diphosphate (FDP) or geranylgeranyl diphosphate (GGDP), products of the mevalonate pathway (Ghittoni et al 2006). Accordingly, depletion of isoprene intermediates linked to reduced *Mvk* activity would be predicted to alter intracellular signalling. Lipid rafts are cholesterol- and glycosphingolipid-rich signalling platforms which amalgamate signalling proteins containing a lipid moiety. For example, major histocompatibility complex class II (MHC II) molecules segregate to lipid raft microdomains in antigen-presenting cells, thus facilitating antigen presentation through a ‘docking platform’ moiety (Ghittoni et al 2006). We predict that intra-cellular depletion of FDP and GGDP or cholesterol may lead to impaired targeting and anchoring of signalling molecules in lipid rafts of *Mvk*<sup>+/-</sup> tissues critical to normal immunological function. Finally, depletion of FDP and GGDP would remove an intracellular regulatory effect on *Mvk* itself, since both isoprenes competitively inhibit *Mvk* activity through binding at the ATP-site of the protein (Hillyard et al 2004; Hinson et al 1997).

In conclusion, our immunological evidence suggests that loss of a single *Mvk* allele in the mouse results in a phenocopy of the human HIDS phenotype. The very recent report of allogeneic bone marrow transplantation in a patient with MA, and the sustained improvement associated with decreased febrile outbreaks and inflammation, serves to highlight the importance of the immunological disturbances we have detected in our model (Neven et al 2007). Our model should have value in exploring pathophysiology associated with human forms of MVK deficiency, including both MA and HIDS, as well as in exploring other autoinflammatory, rheumatic and allergic disorders in which the cholesterol pathway has been implicated.

**Acknowledgement** Gene trap constructs for ablation of murine mevalonate kinase were acquired from Lexicon Pharmaceuticals, The Woodlands, TX, USA. The authors are indebted to Dr Eric Goetzman for helpful discussion and comments on the manuscript, and to Drs Colleen Croniger, Stephen Previs and Henri Brunengraber (Case Western Reserve University, Mouse Metabolic Phenotyping Center) for preliminary characterization of mouse body temperatures.

## References

- Drenth JP, Haagsma CJ, van der Meer JW (1994) Hyperimmunoglobulinemia D and periodic fever syndrome. The clinical spectrum in a series of 50 patients. International Hyper-IgD Study Group. *Medicine* **73**: 133–144.
- Drenth JP, Cuisset L, Grateau G, et al (1999) Mutations in the gene encoding mevalonate kinase cause hyper-IgD and periodic fever syndrome. International Hyper-IgD Study Group. *Nat Genet* **22**: 178–181.
- Ghittoni R, Napolitani G, Benati D, et al (2006) Simvastatin inhibits the MHC class II pathway of antigen presentation by impairing Ras superfamily GTPases. *Eur J Immunol* **36**: 2885–2893.
- Gibson KM, Hoffmann G, Nyhan WL, et al (1988) Mevalonate kinase deficiency in a child with cerebellar ataxia, hypotonia and mevalonic aciduria. *Eur J Pediatr* **148**: 250–252.
- Gibson KM, Gupta M, Baetscher M, Steiner RD, Hoffmann GF, Hager EJ (2006) Early embryonic lethality associated with targeted disruption of the murine mevalonate kinase gene. *J Inherit Metab Dis* **29**(Supplement 1): 50 [abstract].
- Gibson KM, Tse TE, Pappu AS, Steiner RD, Hoffmann GF, Hager EJ (2007) Chronic inflammation and hyper IgD/IgE in mice with targeted deletion of the mevalonate kinase. (*Mvk*) gene. *J Inherit Metab Dis* **30**(Supplement 1): 45 [abstract].
- Hillyard DZ, Jardine AG, McDonald KJ, Cameron AJ (2004) Fluvastatin inhibits raft dependent Fcγ receptor signalling in human monocytes. *Atherosclerosis* **172**: 219–228.
- Hinson DD, Chambliss KL, Toth MJ, Tanaka RD, Gibson KM (1997) Post-translational regulation of mevalonate kinase by intermediates of the cholesterol and nonsterol isoprene biosynthetic pathways. *J Lipid Res* **38**: 2216–2223.
- Hoffmann G, Gibson KM, Brandt IK, Bader PI, Wappner RS, Sweetman L (1986) Mevalonic aciduria—an inborn error of cholesterol and nonsterol isoprene biosynthesis. *N Engl J Med* **314**: 1610–1614.
- Hogema BM, Gupta M, Senephansiri H, et al (2001) Pharmacologic rescue of lethal seizures in mice deficient in succinate semialdehyde dehydrogenase. *Nat Genet* **29**: 212–216.
- Houten SM, Frenkel J, Rijkers GT, Wanders RJ, Kuis W, Waterham HR (2002) Temperature dependence of mutant mevalonate kinase activity as a pathogenic factor in hyper-IgD and periodic fever syndrome. *Hum Mol Genet* **11**: 3115–3124.
- Hubner C, Hoffmann GF, Charpentier C, et al (1993) Decreased plasma ubiquinone-10 concentration in patients with mevalonate kinase deficiency. *Pediatr Res* **34**: 129–133.
- Klasen IS, Goertz JH, van de Wiel GA, Weemaes CM, van der Meer JW, Drenth JP (2001) Hyperimmunoglobulin A in the hyperimmunoglobulinemia D syndrome. *Clin Diagn Lab Immunol* **8**: 58–61.
- Mandey SH, Schneiders MS, Koster J, Waterham HR (2006a) Mutational spectrum and genotype-phenotype correlations in mevalonate kinase deficiency. *Hum Mutat* **27**: 796–802.
- Mandey SH, Kuijk LM, Frenkel J, Waterham HR (2006b) A role for geranylgeranylation in interleukin-1β secretion. *Arthritis Rheum* **54**: 3690–3695.
- Ness GC, Chambers CM (2000) Feedback and hormonal regulation of hepatic 3-hydroxy-3-methylglutaryl coenzyme A reductase: the concept of cholesterol buffering capacity. *Proc Soc Exp Biol Med* **224**: 8–19.
- Neven B, Valayannopoulos V, Quartier P, et al (2007) Allogeneic bone marrow transplantation in mevalonic aciduria. *N Engl J Med* **356**: 2700–2703.
- Ohashi K, Osuga J-i, Tozawa R, et al (2003) Early embryonic lethality caused by targeted disruption of the 3-hydroxy-3-methylglutaryl-CoA reductase gene. *J Biol Chem* **278**: 42936–42941.

- Okamoto T, Fukunaga Y, Ida Y, Kishi T (1988) Determination of reduced and total ubiquinones in biological materials by liquid chromatography with electrochemical detection. *J Chromatogr* **430**: 11–19.
- Pappu AS, Illingworth DR, Bacon S (1989) Reduction in plasma low-density lipoprotein cholesterol and urinary mevalonic acid by lovastatin in patients with heterozygous familial hypercholesterolemia. *Metabolism* **38**: 542–549.
- Pappu AS, Connor WE, Merkens LS, et al (2006) Increased nonsterol isoprenoids, dolichol and ubiquinone, in the Smith–Lemli–Opitz syndrome: effects of dietary cholesterol. *J Lipid Res* **47**: 2789–2798.
- Prietsch V, Mayatepek E, Krastel H, et al (2003) Mevalonate kinase deficiency: enlarging the clinical and biochemical spectrum. *Pediatrics* **111**: 258–261.
- Rios SE, Cho YK, Miziorko HM (2001) Characterization of mevalonate kinase V377I, a mutant implicated in defective isoprenoid biosynthesis and HIDS/periodic fever syndrome. *Biochim Biophys Acta* **1531**: 165–168.
- Tozawa R-i, Ishibashi S, Osuga J-i, et al (1999) Embryonic lethality and defective neural tube closure in mice lacking squalene synthase. *J Biol Chem* **274**: 30843–30848.
- Turpeinen U (1986) Liquid-chromatographic determination of dolichols in urine. *Clin Chem* **32**: 2026–2029.